What controls glycolysis in bloodstream form Trypanosoma brucei?

Bakker, B.M.; Michels, P.A.M.; Opperdoes, F.R.; Westerhoff, H.V.

published in
Journal of Biological Chemistry
1999

DOI (link to publisher)
10.1074/jbc.274.21.14551

document version
Publisher's PDF, also known as Version of record

THE JOURNAL OF BIOLOGICAL CHEMISTRY
Vol. 274, No. 21, Issue of May 21, pp. 14551–14559, 1999

Printed in U.S.A.

What Controls Glycolysis in Bloodstream Form *Trypanosoma brucei*?*

(Received for publication, December 7, 1998, and in revised form, March 3, 1999)

Barbara M. Bakker‡§¶, Paul A. M. Michels‖, Fred R. Opperdoes‖, and Hans V. Westerhoff‡§

From ‡Molecular Cell Physiology, BioCentrum Amsterdam, Vrije Universiteit De Boelelaan 1087, NL-1081 HV Amsterdam, The Netherlands, §E. C. Slater Institute, BioCentrum Amsterdam, University of Amsterdam Plantage Muidergracht 12, NL-1018 TV Amsterdam, The Netherlands, and ‖Research Unit for Tropical Diseases, Christian de Duve Institute of Cellular Pathology and Laboratory of Biochemistry, Catholic University of Louvain, Avenue Hippocrate 74, B-1200 Brussels, Belgium

On the basis of the experimentally determined kinetic properties of the trypanosomal enzymes, the question is addressed of which step limits the glycolytic flux in bloodstream form *Trypanosoma brucei*. There appeared to be no single answer; in the physiological range, control shifted between the glucose transporter on the one hand and aldolase (ALD), glyceraldehyde-3-phosphate dehydrogenase (GAPDH), phosphoglycerate kinase (PGK), and glycerol-3-phosphate dehydrogenase (GDH) on the other hand. The other kinases, which are often thought to control glycolysis, exerted little control; so did the utilization of ATP.

We identified potential targets for anti-trypanosomal drugs by calculating which steps need the least inhibition to achieve a certain inhibition of the glycolytic flux in these parasites. The glucose transporter appeared to be the most promising target, followed by ALD, GDH, GAPDH, and PGK. By contrast, in erythrocytes more than 95% deficiencies of PGK, GAPDH, or ALD did not cause any clinical symptoms (Schuster, R. and Holzhütter, H.-G. (1995) *Eur. J. Biochem.* 229, 403–418). Therefore, the selectivity of drugs inhibiting these enzymes may be much higher than expected from their molecular effects alone. Quite unexpectedly, trypanosomes seem to possess a substantial overcapacity of hexokinase, phosphofructokinase, and pyruvate kinase, making these "irreversible" enzymes mediocre drug targets.

Trypanosoma brucei is a unicellular, eukaryotic parasite. It causes the African sleeping sickness in humans and a related disease, nagana, in livestock. When this organism lives in the mammalian bloodstream, it depends completely on glycolysis for its supply of ATP. It possesses neither a functional Krebs cycle nor oxidative phosphorylation, nor does it store any carbohydrate. Glycolysis in trypanosomes and in other members of the Kinetoplastida family differs substantially from the corresponding pathway in other organisms (for reviews see Refs. 1–4). First, the conversion of glucose to 3-phosphoglycerate (3-PGA)[1] takes place in specialized organelles, related to peroxisomes. Since 90% of the protein content of these organelles consists of glycolytic enzymes, they have been called glycosomes (5). The glycosomal membrane is hardly permeable to metabolites (6). Second, under aerobic conditions, the NADH produced in glycolysis is reoxidized by molecular oxygen via a mitochondrial glycerol 3-phosphate:DHAP (Gly-3-P:DHAP) shuttle (Fig. 1). Since there is neither a cytosolic glycerol kinase (GK) nor any significant activity of glycerol 3-phosphatase (5, 7), all Gly-3-P is shuttled back via DHAP to the mitochondria and converted to pyruvate, leading to the production of two molecules of pyruvate per molecule of glucose consumed. Under anaerobic conditions, equimolar amounts of pyruvate and glycerol are produced due to requirements of glycosomal redox and ATP balance (1, 5, 7–10). This decreases the ATP production to one molecule of ATP per glucose. Third, the glycosomal enzymes are hardly regulated by any of the compounds that strongly affect the corresponding enzymes in other organisms. Most notably, in trypanosomes, fructose 2,6-bisphosphate activates the cytosolic enzyme PYK (11–13) rather than the glycosomal PFK (14, 15). The physiological function of this activation is elusive, since the fructose 2,6-bisphosphate concentration in the bloodstream form substantially exceeds its activation constant for PYK (12, 16).

It has been suggested that the transport of glucose into the cells is the rate-limiting step of glycolysis in bloodstream form trypanosomes (17). Yet, our present day knowledge of control of metabolism led us to re-evaluate the evidence for this statement (4). Since the development of metabolic control analysis (18, 19) (for reviews, see Refs. 20 and 21), it has been known that in general there is no single rate-limiting step in a metabolic pathway, but control can be shared among several steps. The quantitative measure of the strength of the control of the steady-state flux J through a pathway by an enzyme i in this pathway is given by its flux control coefficient, C_i^J. This coefficient is defined as the percentage increase of the flux caused by a 1% activation of enzyme i (for a more precise definition see Refs. 22 and 23). Flux control coefficients can have any value

* This study was supported by the Netherlands Organization for Scientific Research and the Netherlands Association of Biotechnology Research Schools. The costs of publication of this article were defrayed in part by the payment of page charges. This article must therefore be hereby marked "*advertisement*" in accordance with 18 U.S.C. Section 1734 solely to indicate this fact.

¶ Present address: Kluyver Laboratory for Biotechnology, Delft University of Technology, Julianalaan 67, NL-2628 BC Delft, The Netherlands.

** To whom correspondence should be addressed: Molecular Cell Physiology, BioCentrum Amsterdam, Vrije Universiteit De Boelelaan 1087, NL-1081 HV Amsterdam, The Netherlands. Tel.: 31 20 4447228; Fax: 31 20 4447229; E-mail: hw@bio.vu.nl.

[1] The abbreviations used are: PGA, phosphoglycerate; ALD, fructose-1,6-bisphosphate aldolase; 1,3-BPGA, 1,3-bisphosphoglycerate; subscript c and g, cytosolic and glycosomal, respectively; C_i^J, flux control coefficient of enzyme i; DHAP, dihydroxyacetone phosphate; $\varepsilon_{X_j}^i$, elasticity coefficient of enzyme i for metabolite j; Fru-1,6-BP, fructose 1,6-bisphosphate; Fru-6-P, fructose 6-phosphate; Γ, ratio of product and substrate concentrations; GA-3-P, glyceraldehyde 3-phosphate; GAPDH, glyceraldehyde-3-phosphate dehydrogenase; GDH, glycerol-3-phosphate dehydrogenase; GK, glycerol kinase; Gly-3-P, glycerol 3-phosphate; Glc-6-P, glucose 6-phosphate; HK, hexokinase; J, steady-state flux; K_{eq}, equilibrium constant; P-enolpyruvate, phosphoenolpyruvate; PFK, phosphofructokinase; PGK, phosphoglycerate kinase; PYK, pyruvate kinase; TIM, triosephosphate isomerase; V, volume.

between 0 (not limiting) and 1 (completely rate-limiting) (*e.g.* Refs. 24–28), but the sum of the flux control coefficients of all enzymes in the pathway should be 1 (18).

To measure a flux control coefficient, it is necessary to modulate the activity of the enzyme of interest with small steps around the normal wild type level. For the trypanosome glucose transporter, this has not been done. Consequently, the evidence presented for the glucose transporter being rate-limiting is only indirect and qualitative. In the first place, glucose, fructose, and mannose were metabolized at different rates (17). However, the comparison of different substrates alone did not correspond to the small modulation required for metabolic control analysis. In addition, the modulation of the transport activity was not quantified, nor did this experiment exclude control by phosphorylation. Also the low intracellular glucose concentration (0.4 mM) has been taken as evidence that glucose transport was rate-limiting (29). However, a theoretical analysis, based on the kinetics of the glucose transporter and of HK, showed that an intracellular glucose concentration of 0.4 mM may be consistent with any flux control coefficient between 0 and 50%, but not 100% (4). This suggests that, if at all important, glucose transport is not the only step controlling trypanosome glycolysis.

Because bloodstream form trypanosomes depend completely on glycolysis for their supply of ATP and because the organization of glycolysis in the parasite is very different from that in the host cells, this pathway has been selected as a target for drugs against the African sleeping sickness (30). The selectivity of drugs might be enhanced by choosing a target enzyme that has a high control in the parasite and a low control in the host.

Despite the great interest, it is not yet known completely for any organism how the control of the glycolytic flux is distributed. In yeast, for example, many genes encoding glycolytic enzymes (HK, phosphoglucose isomerase, PGK, PYK, pyruvate decarboxylase, alcohol dehydrogenase) have been overexpressed manifold, but in none of the mutants did the glycolytic flux differ substantially from the wild type flux (31, 32). This may be due to several reasons. First, glycolysis in yeast (and many other organisms) is part of a much wider metabolic network. Consequently, the glycolytic flux may be controlled by steps outside glycolysis, such as the utilization of ATP, the respiratory branch, the synthesis of storage carbohydrates, and/or the glucose transporter proteins (33). Second, the effects of overexpression are necessarily investigated at time scales at which the cells may adjust the expression of other genes. For example, the PFK-overproducing cells contained decreased levels of 6-phosphofructo-2-kinase. Thus, they compensated for the increased amount of PFK by decreasing the concentration of its activator fructose 2,6-bisphosphate (32). Finally, when the activity of an enzyme is increased, it often (but not always) loses control (34). By using overexpression mutants, one therefore runs the risk of underestimating the control coefficients.

Several studies dealt with the control of glucose utilization in mammalian cells. Measurements indicated that the rate of glycogen synthesis was controlled by glucose transport and hexokinase (35). The control of mammalian glycolysis has been measured by the so-called matrix inversion method (36). In the absence of insulin, most control was shared by glucose transport and hexokinase. This method, however, requires that all relevant enzymes be included, but important steps such as PFK and GAPDH were missing.

The above mentioned problems with the determination of control coefficients should not apply, or should apply to a lesser extent, to bloodstream form *T. brucei*. First, except for the utilization of ATP, there are no branches with a substantial flux under aerobic conditions. Second, the kinetics of glycolytic enzymes from *T. brucei* have been investigated thoroughly in a limited number of laboratories under standard conditions. This has enabled us to develop a detailed kinetic model of trypanosome glycolysis containing most glycolytic enzymes. The model calculations of the flux and the metabolite concentrations corresponded unexpectedly well with experimental information (37). We here use the kinetic data to calculate what controls trypanosome glycolysis under physiological conditions. It will be shown that there is a distribution of control of trypanosome glycolysis, which depends strongly on glucose supply.

MATERIALS AND METHODS

Cultivation of Trypanosomes

All experiments were performed with the bloodstream form of *T. brucei* stock 427. Male, 300-g Wistar rats were infected with *T. brucei*, and the parasites were isolated from the blood by DEAE-cellulose chromatography (DE52, Whatman) (38). The cells were washed by centrifugation; resuspended in a 90 mM Tris/HCl buffer containing 2.5 mM KCl, 77.5 mM NaCl, 5 mM $MgCl_2$, 2 mM Na_2HPO_4, and 50 mM glucose at pH 7.5 (modified from Ref. 39); and stored on ice. In this buffer, the cells maintained a constant motility and oxygen consumption capacity for at least 7 h after isolation.

Flux and Metabolite Measurements

An aliquot of cells was washed three times by centrifugation at 4 °C and resuspended in the assay buffer at 37 °C. The measurements were performed in a 90 mM Tris/HCl buffer (pH 7.5), containing 3.1 mM KCl, 96.9 mM NaCl, 5 mM $MgCl_2$, 2 mM Na_2HPO_4, and the indicated concentration of glucose. The protein concentration was measured in each aliquot of cells, according to Lowry (40) with bovine serum albumin as a standard. Since the buffer weakly disturbed the assay, the same amount of buffer as present in the samples was added to the bovine serum albumin standards.

The rate of oxygen consumption was monitored in a closed and thermostated vessel with a Clark electrode. For determination of the concentrations of other metabolites, the cells were kept in an open, thermostated vessel and aerated with water-saturated pressurized air. To check that the cell suspensions remained aerobic, the oxygen concentration was monitored with a Clark electrode throughout the experiment. Samples were taken by injecting 75 μl of the cell suspension into 37.5 μl of 15% perchloric acid. Samples were vortexed, centrifuged (5 min, Eppendorf table centrifuge, full speed), neutralized by mixing 80 μl of supernatant with 45 μl of 1 M K_2CO_3, and centrifuged again. The pH of the supernatants was checked with pH paper (pH was between 7 and 8). Supernatants were stored at −20 °C and analyzed further within 1 week. Glucose, pyruvate, and glycerol were measured by NADH-linked analysis (41) in an automatic analyzer (COBAS FARA, Roche Molecular Biochemicals).

Chemicals

Phloretin was from Sigma. A phloretin stock was made up in 70% ethanol. The ethanol concentration in cell suspensions was always kept below 1%.

Modeling

The kinetic model of trypanosome glycolysis that was used in this study has been described and validated previously, its predictions being compared with experimental results (37). It contained enzyme kinetics, measured with purified trypanosome enzymes, for most reactions depicted in Fig. 1. The reactions catalyzed by phosphoglucose isomerase, triosephosphate isomerase (TIM), phosphoglycerate mutase, enolase, and adenylate kinase were taken to be at equilibrium. The rationale was that their measured ratios of substrate and product concentrations were close to equilibrium (phosphoglycerate mutase and enolase) (42), that they catalyze a dead-end branch (adenylate kinase), or that they were close to equilibrium in initial model calculations with explicit kinetics for these reactions (phosphoglucose isomerase and TIM). The glycosomal membrane was assumed to be impermeable to metabolites (6), except to those that need to be transported to allow glycolysis to proceed. Because of a lack of kinetic information, the latter transport steps were assumed to be at equilibrium. The transport of glucose across the cytoplasmic and subsequently the glycosomal membranes was lumped into one kinetic equation, because no distinction could be made so far (29, 43). This is equivalent to assuming the glycosomal glucose transporter to be at equilibrium. The glycosomal concentration of inorganic phosphate was assumed to be saturating. This assumption

has been validated partially. At the normal blood concentration of inorganic phosphate (0.4–0.5 mM (44)), the measured rate of oxygen consumption by intact trypanosomes, *i.e.* the glycolytic flux, was fully saturated with phosphate (result not shown).

The concentrations of both the adenine nucleotides (ATP, ADP, AMP) and the nicotinamide adenine nucleotides (NAD, NADH) were treated as free (although interdependent) variables, rather than fixed parameters of the system. Due to the compartmentalization of the pathway, the model contained distinct pools of cytosolic and glycosomal adenine nucleotides. In principle, the model allowed both dynamic and steady-state calculations, but the present study is limited to steady states only. Below, only the changes that were made to the model described in Ref. 37 are described.

Kinetics—The kinetics of GDH have been determined more accurately[2]: K_m, DHAP = 0.1 mM; K_m, Gly-3-P = 2 mM; K_m, NADH = 0.01 mM; K_m, NAD+ = 0.4 mM; and the ratio of the reverse and forward V_{max} (V^-/V^+) = 0.28. The specific activity of the purified enzyme in the forward direction was 213 μmol min^{-1} (mg of enzyme)$^{-1}$. The amount of GDH in the cell is 0.25% of the total cell protein (45). Expressed per total cell protein, V^+ is then 533 nmol min^{-1} mg of protein^{-1}.

Bakker *et al.* (37) took the hexose kinases to be insensitive to their products. Originally only an indirect and weak effect of glucose 6-phosphate (Glc-6-P) on HK and of fructose 1,6-bisphosphate (Fru-1,6-BP) on PFK was included in the model via the conservation relation of bound phosphates. Under some conditions, this might cause the set of equations defining the steady state to be underdetermined. This would be the case, for instance, if ALD were saturated with Fru-1,6-BP. Then none of the enzymes would sense the concentration of Fru-1,6-BP, and consequently the latter could assume any value, only restricted by the conserved sum. It has been reported that Fru-1,6-BP does inhibit PFK, by acting both on the V_{max} and the K_m for Fru-6-P (14). In the present study the following rate equation was used,

$$\nu_{PFK} = V^+ \cdot \left(\frac{K_{i1}}{[\text{Fru-1,6-BP}] + K_{i1}}\right) \cdot \left(\frac{\frac{[\text{Fru-6-P}]}{K_{m,\text{Fru-6-P}}}}{1 + \frac{[\text{Fru-6-P}]}{K_{m,\text{Fru-6-P}}} + \frac{[\text{Fru-1,6-BP}]}{K_{i2}}}\right) \cdot \left(\frac{\frac{[\text{ATP}]}{K_{m,\text{ATP}}}}{1 + \frac{[\text{ATP}]}{K_{m,\text{ATP}}}}\right) \quad \text{(Eq. 1)}$$

in which K_{i1} = 15.8 mM and K_{i2} = 10.7 mM (14). All other parameters held the same values as described previously (37). HK was reported to be insensitive to Glc-6-P (46). Due to salt effects and a high affinity of the enzyme for glucose (K_m = 0.1 mM), a competitive inhibition by Glc-6-P with a K_m above 10 mM would not be measurable.[3] Under some conditions, such a weak inhibition was relevant to prevent unrestrained accumulation of Glc-6-P in the model, and therefore the rate equation was modified to the following equation.

$$\nu_{HK} = V^+ \cdot \left(\frac{\frac{[\text{Glc}]}{K_{m,\text{Glc}}}}{1 + \frac{[\text{Glc}]}{K_{m,\text{Glc}}} + \frac{[\text{Glc-6-P}]}{K_{m,\text{Glc-6-P}}}}\right) \cdot \left(\frac{\frac{[\text{ATP}]}{K_{m,\text{ATP}}}}{1 + \frac{[\text{ATP}]}{K_{m,\text{ATP}}} + \frac{[\text{ADP}]}{K_{m,\text{ADP}}}}\right) \quad \text{(Eq. 2)}$$

$K_{m,\text{Glc-6-P}}$ was taken to be 12 mM, which does not contradict the measurements. The other parameters were not changed (37).

The rate of PYK was assumed to be independent of the concentrations of its products, ADP and pyruvate, unless otherwise mentioned. If the rate depended on the ATP concentration, the following rate equation was used.

$$\nu_{PYK} = V^+ \cdot \left(\frac{\left(\frac{[\text{P-enolpyruvate}]}{K_{m,\text{P-enolpyruvate}}}\right)^n}{1 + \left(\frac{[\text{P-enolpyruvate}]}{K_{m,\text{P-enolpyruvate}}}\right)^n}\right) \cdot \left(\frac{\frac{[\text{ADP}]_c}{K_{m,\text{ADP}}}}{1 + \frac{[\text{ADP}]_c}{K_{m,\text{ADP}}} + \frac{[\text{ATP}]_c}{K_{m,\text{ATP}}}}\right) \quad \text{(Eq. 3)}$$

$K_{m,\text{ATP}}$ was taken to be 0.1 mM (equal to $K_{m,\text{ADP}}$ (47)), and the other parameter values were not changed (37).

Non-competitive inhibition of glucose transport was simulated by multiplying the rate equation for glucose transport by a factor $K_i/(K_i + [\text{I}])$, in which [I] represents the inhibitor concentration and K_i is the inhibition constant. Competitive inhibition of glucose transport was simulated by multiplying the K_m values for both extracellular and intracellular glucose by a factor $1 + [\text{I}]/K_i$.

[2] S. Marché, F. R. Opperdoes, and P. A. M. Michels, unpublished results.

[3] J. van Roy and F. R. Opperdoes, unpublished results.

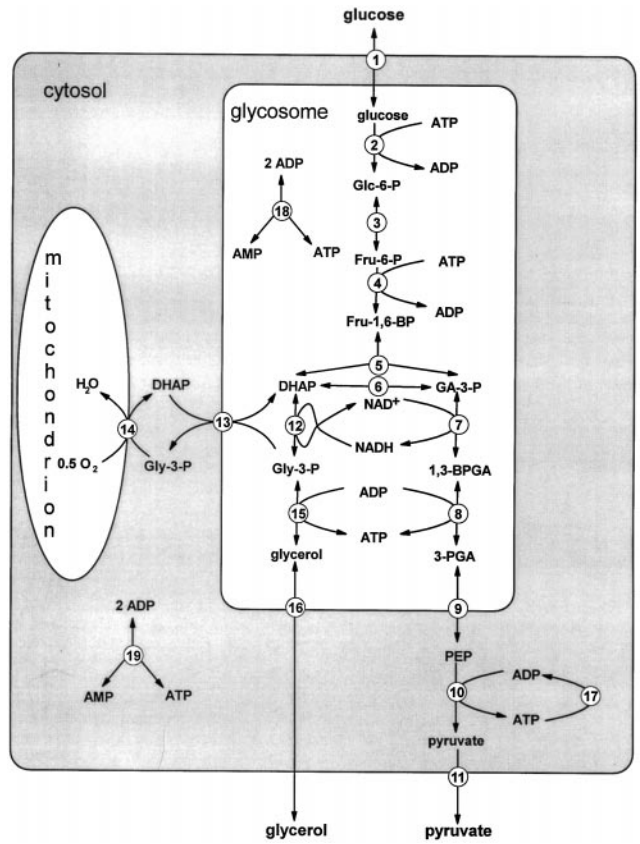

FIG. 1. **The stoichiometric scheme of the model of glycolysis in bloodstream form *T. brucei*.** The reactions *3*, *6*, *9*, *13*, *16*, *18*, and *19* were treated as equilibrium reactions. *1*, transport of glucose across the plasma membrane and the glycosomal membrane; *2*, HK; *3*, phosphoglucose isomerase; *4*, PFK; *5*, ALD; *6*, TIM; *7*, GAPDH; *8*, PGK; *9*, transport of 3-PGA across the glycosomal membrane, phosphoglycerate mutase, and enolase; *10*, PYK; *11*, pyruvate transport across the plasma membrane; *12*, GDH; *13*, transport of Gly-3-P and DHAP across the glycosomal membrane; *14*, glycerol-3-phosphate oxidase; *15*, GK; *16*, transport of glycerol across the glycosomal membrane and the plasma membrane; *17*, ATP utilization; *18*, glycosomal adenylate kinase; *19*, cytosolic adenylate kinase. *PEP*, P-enolpyruvate.

The Transport of Gly-3-P and DHAP—Under anaerobic conditions, bloodstream form *T. brucei* maintains its glycosomal redox and ATP balance by producing equimolar amounts of pyruvate and glycerol (Fig. 1). The $\Delta G^{0\prime}$ of GK does not favor the production of glycerol. An inhibition of glycolysis by glycerol has indeed been measured under anaerobic conditions (48). In the original kinetic model (37), the concentration of glycerol required to inhibit the flux was much lower than had been found experimentally. The model assumed the transport of Gly-3-P and DHAP across the glycosomal membrane to be independent of each other and at equilibrium. Consequently, any increase of the glycosomal concentration of Gly-3-P was accompanied by an identical increase of the cytosolic concentration of Gly-3-P. Both the cytosolic and the glycosomal concentration of Gly-3-P participated in a conserved sum of organic phosphate groups that are not exchanged with inorganic phosphate as follows,

$$[\text{Gly-3-P}]_g V_g + [\text{Gly-3-P}]_c V_c + [\text{DHAP}]_g V_g + [\text{DHAP}]_c V_c + [\text{Glc-6-P}]_g V_g + [\text{Fru-6-P}]_g V_g + 2[\text{Fru-1,6-BP}]_g V_g + [\text{GA-3-P}]_g V_g + [\text{1,3-BPGA}]_g V_g + 2[\text{ATP}]_g V_g + [\text{ADP}]_g V_g = C_4 \cdot V_g \quad \text{(Eq. 4)}$$

in which V_g is the glycosomal volume and V_c is the cytosolic volume. Since the cytosolic volume was more than 20 times the glycosomal volume, any increase of the cytosolic Gly-3-P concentration led to an enormous drain of the glycosomal metabolites. This effect enhanced the inhibition of the anaerobic glycolytic flux by glycerol.

If the transport of Gly-3-P and DHAP would occur via an antiport mechanism, as proposed by Opperdoes and Borst (5), the conserved sum of bound phosphates would split in distinct glycosomal and cytosolic conserved sums.

$$[\text{Gly-3-P}]_g + [\text{DHAP}]_g + [\text{Glc-6-P}]_g + [\text{Fru-6-P}]_g + 2[\text{Fru-1,6-BP}]_g + [\text{GA-3-P}]_g + [\text{1,3-BPGA}]_g + 2[\text{ATP}]_g + [\text{ADP}]_g = C_{4,\text{antiporter}} \quad \text{(Eq. 5)}$$

and

$$[\text{Gly-3P}]_c + [\text{DHAP}]_c = C_{5,\text{antiporter}} \quad \text{(Eq. 6)}$$

Consequently, an increase of the glycosomal Gly-3-P concentration would not be automatically coupled to an equal increase of the cytosolic Gly-3-P concentration. Therefore, it was expected that the inhibition of anaerobic glycolysis by glycerol would be much weaker. This hypothesis was tested by implementing a Gly-3-P:DHAP antiporter in the model.

It was assumed that the antiporter was in equilibrium. Also, TIM was taken to be in equilibrium, as previously. Therefore, the triosephosphates were considered to behave as a single metabolite pool.

$$[\text{triose-P}] \equiv \frac{[\text{DHAP}]_c V_c + [\text{DHAP}]_g V_g + [\text{GA-3-P}]_g V_g}{V_{\text{tot}}} \quad \text{(Eq. 7)}$$

The time derivative of [triose-P] remained exactly the same as in the model with the two independent transporters (37). The implementation of the antiporter entailed the solving of a set of five equations with five unknowns, *i.e.* Equations 5–7 and the equilibrium constraints for TIM and the exchanger itself.

$$\frac{[\text{GA-3-P}]_g}{[\text{DHAP}]_g} = K_{eq,\text{TIM}} \quad \text{(Eq. 8)}$$

$$\frac{[\text{Gly-3-P}]_c[\text{DHAP}]_g}{[\text{Gly-3-P}]_g[\text{DHAP}]_c} = K_{eq,\text{antiporter}} = 1 \quad \text{(Eq. 9)}$$

It follows that the cytosolic DHAP concentration is as follows,

$$[\text{DHAP}]_c = \frac{-b + \sqrt{b^2 - 4ac}}{2a} \quad \text{(Eq. 10)}$$

in which

$$a = K_{eq,\text{TIM}} \cdot \frac{V_c}{V_g} \quad \text{(Eq. 11)}$$

$$b = Q \cdot (1 + K_{eq,\text{TIM}}) + \frac{V_c}{V_g} \cdot C_{5,\text{antiporter}} - [\text{triose-P}] \cdot \left(1 + \frac{V_c}{V_g}\right) \cdot K_{eq,\text{TIM}} \quad \text{(Eq. 12)}$$

$$c = -[\text{triose-P}] \cdot \left(1 + \frac{V_c}{V_g}\right) \cdot C_{5,\text{antiporter}} \quad \text{(Eq. 13)}$$

and

$$Q = [\text{DHAP}]_g + [\text{GA-3-P}]_g + [\text{Gly-3-P}]_g = C_{4,\text{antiporter}} - [\text{Glc-6-P}]_g - [\text{Fru-6-P}]_g - 2[\text{Fru-1,6-BP}]_g - [\text{1,3-PGA}]_g - 2[\text{ATP}]_g - [\text{ADP}]_g \quad \text{(Eq. 14)}$$

When $[\text{DHAP}]_c$ was known, $[\text{DHAP}]_g$ followed from equations 5, 6, 8, and 9.

$$[\text{DHAP}]_g = \frac{Q \cdot [\text{DHAP}]_c}{C_{5,\text{antiporter}} + K_{eq,\text{TIM}} \cdot [\text{DHAP}]_c} \quad \text{(Eq. 15)}$$

Subsequently, $[\text{Gly-3-P}]_c$, $[\text{GA-3-P}]_g$, and $[\text{Gly-3-P}]_g$ were calculated from Equations 6, 8, and 9, respectively. All other equations in the model were as specified in Ref. 37. The values of $C_{4,\text{antiporter}}$ and the sum of the glycosomal adenine nucleotides (C_1) have not been determined experimentally. They were chosen as follows: $C_1 = 6$ mM, and $C_{4,\text{antiporter}} = 45$ mM. $C_{5,\text{antiporter}}$ (5 mM) was based on measurements of average concentrations of Gly-3-P and DHAP in the cell (42). To allow comparison of the model with and without the antiport mechanism, the total amount of metabolites contained in C_4 on the one hand and $C_{4,\text{antiporter}}$ and $C_{5,\text{antiporter}}$ on the other hand was kept the same, as follows.

$$C_4 = C_{4,\text{antiporter}} + (V_c/V_g) \cdot C_{5,\text{antiporter}} = 156.5 \text{ mM} \quad \text{(Eq. 16)}$$

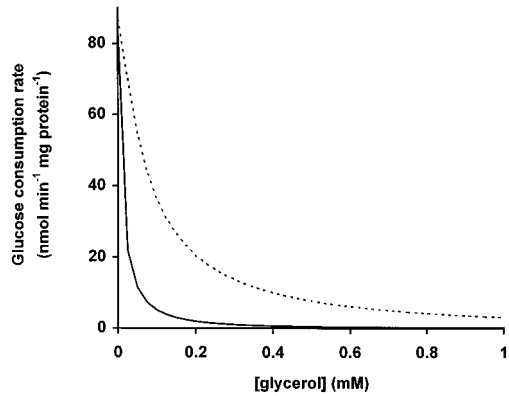

FIG. 2. **The inhibition of the glycolytic flux by glycerol under anaerobic conditions depends on the stoichiometry of the transport of Gly-3-P and DHAP.** The *solid line* represents the inhibition curve that was calculated, if it was assumed that these metabolites were transported independently across the glycosomal membrane. The *dashed line* is the corresponding curve if their transport was coupled by an antiporter. Details of the model can be found under "Materials and Methods."

Indeed, the coupling of the transport of Gly-3-P and DHAP transport made the anaerobic flux less sensitive to glycerol (Fig. 2). The $K_{0.5}$ of glycerol increased 7.5-fold from 10 μM (independent transport) to 75 μM (antiporter). Nevertheless, the calculated $K_{0.5}$ was still lower than the measured $K_{0.5}$ (800 μM) (48). Table I shows that the implementation of the antiporter did not cause a substantial deviation of the model from the experiments with regard to the flux and the metabolite concentrations as far as they could be measured in cell extracts (42). Only the modeled concentration of DHAP deviated more than 3-fold from the experiments due to the antiporter, while it was correctly predicted if the transport was uncoupled. The results that will be shown have been obtained with a Gly-3-P:DHAP antiporter. It was confirmed that these results were virtually independent of the mechanism of transport.

Quantifying Control—The control of an enzyme i on a steady-state flux J was defined by its flux control coefficient,

$$C_i^J = \frac{(d\ln J/dp)}{(\partial \ln \nu/\partial p)} \cdot 100\% = \frac{\nu}{J} \cdot \frac{(dJ/dp)}{(\partial \nu/\partial p)} \cdot 100\% \quad \text{(Eq. 17)}$$

in which ν is the rate of enzyme i, p is a parameter that only affects enzyme i, and $(\partial \nu/\partial p)$ is the effect of the parameter change on ν if the enzyme were isolated from the rest of the metabolic pathway, *i.e.* at constant concentrations of all metabolites. The flux control coefficient of an enzyme or transporter was calculated numerically by increasing its forward (V^+) and reverse (V^-) maximal rate in proportion by 0.01% and calculating the steady-state flux J both prior to and after this change. C_i^J was evaluated as follows.

$$C_i^J = \frac{\Delta J}{\Delta V^+} \cdot \frac{V^+}{J} \cdot 100\% \quad \text{(Eq. 18)}$$

It has always been verified that the results obeyed the summation theorem,

$$\sum C_i^J = 100\% \quad \text{(Eq. 19)}$$

in which the summation is over all enzymes i in the pathway.

The sensitivity of an enzyme to a metabolite concentration was evaluated in terms of its elasticity coefficient, defined by the equation,

$$\varepsilon_{X_j}^i = \frac{X_j}{\nu_i} \cdot \frac{\partial \nu_i}{\partial X_j} \quad \text{(Eq. 20)}$$

in which X_j is the concentration of metabolite j. Partial derivatives were taken at constant concentrations of the other metabolites at their steady-state values. Numerically, elasticity coefficients were determined by calculating ν_i and X_j in the steady state, increasing X_j by 0.01%, and calculating the change of ν_i.

Control coefficients and elasticity coefficients are related by connectivity theorems. The connectivity theorem for intracellular glucose is, for example, the following.

$$C^J_{\text{glucose transport}} \cdot \varepsilon^{\text{glucose transport}}_{\text{Glc}_i} + C^J_{\text{HK}} \cdot \varepsilon^{\text{HK}}_{\text{Glc}_i} = 0 \quad \text{(Eq. 21)}$$

TABLE I

The measured and calculated glycolytic flux and metabolite concentrations

The steady-state glycolytic flux and metabolite concentrations, as they were calculated with independent transport of Gly-3-P and DHAP or with an antiporter, are compared with experimental values (42). The ratios of aerobic to anaerobic concentrations were taken to avoid inaccuracy due to the conversion of amounts measured in nmol/mg wet weight to intracellular concentrations in mM. Since the measured concentrations represent a weighted average of glycosomal and cytosolic concentrations, this average was also used for the [DHAP] and [Gly-3-P] calculated by the model. The ratio of cytosolic and glycosomal volume was 22.3. Rates are expressed in nmol min^{-1} mg of $protein^{-1}$, and concentrations are in mM. When experimental data are available for comparison, boldface numbers are used.

	Independent transport of Gly-3-P and DHAP			Gly-3-P:DHAP antiporter			Measured ratio
	Aerobic	Anaerobic	Ratio	Aerobic	Anaerobic	Ratio	
Glucose consumption rate	74	74	**1.0**	74	75	**0.99**	**1**
ATP/ADP_c	3.0	1.5	**2.0**	3.0	1.5	**2.0**	**2.4**
ATP/ADP_g	1.0	0.63	1.6	0.94	1.7	0.55	
$DHAP_c$	1.1	0.41	2.7	1.5	0.17	8.82	
$DHAP_g$	1.1	0.41	2.7	1.1	0.67	1.6	
$DHAP_{average}$	1.1	0.41	**2.7**	1.5	0.20	**7.5**	**2.3**
3-PGA	0.68	0.47	**1.5**	0.69	0.47	**1.5**	**4.1**
2-PGA	0.13	0.087	**1.5**	0.13	0.088	**1.5**	**1.8**
P-enolpyruvate	0.86	0.58	**1.5**	0.86	0.59	**1.5**	**1.9**
$Gly\text{-}3\text{-}P_c$	3.5	5.8	0.6	3.5	4.8	0.73	
$Gly\text{-}3\text{-}P_g$	3.5	5.8	0.6	2.6	19.7	0.13	
$Gly\text{-}3\text{-}P_{average}$	3.5	5.8	**0.6**	3.5	5.7	**0.61**	**0.25**

This means that the process that is the more sensitive to intracellular glucose has the lower control. This can be understood intuitively, because the more sensitive process tends to adapt to a change elsewhere in the system.

If specific conditions are fulfilled (49), a group of enzymes may be treated as a single module. Under "The Distribution of Control between the Supply and Demand for ATP" below, this principle was applied. The glycolytic pathway was simplified to two modules: one producing cytosolic ATP (supply) and one consuming it (demand) (20, 50, 51). For this system, the following modular connectivity theorem holds,

$$C^J_{\text{supply}} \cdot {}^*\varepsilon^{\text{supply}}_{[ATP]_c/[ADP]_c} + C^J_{\text{demand}} \cdot {}^*\varepsilon^{\text{demand}}_{[ATP]_c/[ADP]_c} = 0 \qquad \text{(Eq. 22)}$$

in which the asterisk emphasizes that these elasticities apply to the whole module rather than to a single reaction. The summation theorem for the flux control coefficients remains as follows.

$$C^J_{\text{supply}} + C^J_{\text{demand}} = 100\% \qquad \text{(Eq. 23)}$$

Together, Equations 22 and 23 yield the following.

$$C^J_{\text{demand}} = \frac{100\%}{1 - \frac{{}^*\varepsilon^{\text{demand}}_{[ATP]_c/[ADP]_c}}{{}^*\varepsilon^{\text{supply}}_{[ATP]_c/[ADP]_c}}} \qquad \text{(Eq. 24)}$$

Usually, ${}^*\epsilon^{\text{supply}}_{[ATP]_c/[ADP]_c}$ is negative (product inhibition), and ${}^*\epsilon^{\text{demand}}_{[ATP]_c/[ADP]_c}$ is positive, so that C^J_{demand} is between 0 and 100%. To calculate the control of PYK on the flux through the supply module ($C^{J\ \text{supply}}_{\text{PYK}}$), the cytosolic [ATP]/[ADP] ratio was fixed.

Substrate and Product Concentrations—The extracellular concentrations of glucose, pyruvate, and glycerol were kept constant at 5, 0, and 0 mM, respectively, unless mentioned otherwise.

Software—Conserved sums were analyzed with the program SCAMP (52). The simulations were performed with MLAB (Civilized Software, Bethesda, MD).

RESULTS

The Control of the Glycolytic Flux under Physiological Conditions—The first question we addressed was which reactions or transport steps control the glycolytic flux of trypanosomes in the mammalian bloodstream. Although the mammalian bloodstream is a very constant environment in many respects, the cells may encounter extracellular glucose concentrations varying between 4 and 8 mM (53, 54). The oxygen concentration is saturating throughout the vascular system (4). Under aerobic conditions, only a very small rate of glycerol production was measured (Table II); therefore, the branch to glycerol was neglected in all aerobic simulations reported here (see also Ref. 37). It was calculated to which extent glucose transport limits

TABLE II

The fluxes as measured under aerobic conditions at 37 °C

Note that the measured fluxes were higher than the calculated fluxes (Table I), since the model refers to 25 °C (37).

Substrate	Flux (nmol min^{-1} mg of $protein^{-1}$) or flux ratio
Glucose	−152
Pyruvate	339
Glycerol	7
O_2	−158 ± 11
$J_{O2}/J_{\text{glucose}}$	1.0
$J_{\text{pyruvate}}/J_{\text{glucose}}$	−2.2
$J_{\text{glycerol}}/J_{\text{glucose}}$	0.0

glycolysis under these conditions. Whereas glucose transport controlled the flux at low extracellular glucose concentrations, control gradually eluded the transporter at the higher glucose concentrations, to be taken over by ALD, GAPDH, PGK, and GDH together (Fig. 3). In accordance with the concepts of metabolic control analysis, the control was condition-dependent and was shared by several steps at high glucose concentrations. Furthermore, there was no relationship whatsoever between the extent to which any of the enzymes controlled the glycolytic flux and its distance from equilibrium (Table III). At 5 mM glucose, the glucose transporter controlled the flux for more than 90%, but the irreversible enzymes HK, PFK, and PYK were much further displaced from equilibrium than the transporter.

The Control by Glucose Transport Is Highly Variable—The above calculations depend on many kinetic parameters, all of which have been measured with finite accuracy and some of which may be subject to biological variation or regulation. Therefore, the sensitivity of the results to inaccuracies in the parameter values has been investigated by varying the V_{max} values of all enzymes around their default values at 5 mM glucose. It turned out that most flux control coefficients depended weakly on the enzyme activities around their measured values. A most surprising exception was the flux control by the glucose transporter, which depended strongly on the activities of various processes. Under aerobic conditions, a relatively small increase of the activity of the transporter above the measured value already caused its flux control coefficient to drop to 0 (Fig. 4). Also, reduction of the V_{max} of ALD, GAPDH, or PGK shifted the control from the transporter to other

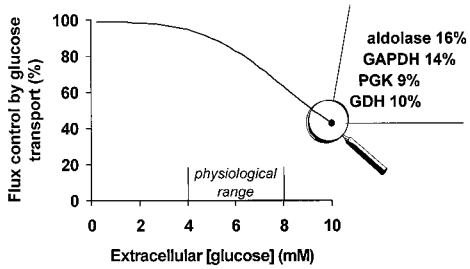

FIG. 3. **The flux control coefficient of the glucose transporter depends on the extracellular glucose concentration.** This result was obtained under aerobic conditions. The *inset* shows the flux control coefficients of those enzymes that take over control, when the transporter loses control at 10 mM glucose.

enzymes.

In view of the uncertainty of the exact V_{max} of the glucose transporter and possible variation between trypanosome populations or between individual cells within populations, it is hard to predict where in the curve of Fig. 4 a trypanosome will be. What *can* be predicted is which enzymes do control the flux at increased transport activities. To this end, the transport activity was increased by 35%, and the flux control distribution was calculated again. Under aerobic conditions, ALD, GAPDH, PGK, and GDH assumed most of the control, and again there was no relationship between the flux control coefficients and the displacement from equilibrium (Table IV). Under anaerobic conditions, the V_{max} of the glucose had to be doubled before the transporter lost all control (Fig. 4). Then ALD, GAPDH, PGK, GDH, and GK together took over control (result not shown).

Experimental Determination of the Sensitivity of the Glycolytic Flux to Inhibition of Glucose Transport—Since modeling alone was not sufficient to decide whether or not glucose transport controlled the glycolytic flux, additional experiments were carried out. Glucose transport was inhibited by increasing concentrations of phloretin, and the rate of oxygen consumption was measured at 0.5 and 5 mM glucose (Fig. 5, *circles*). The rate of oxygen consumption is a measure of the glycolytic flux, since bloodstream form trypanosomes consume one molecule of oxygen per molecule of glucose under aerobic conditions (Table II).

Phloretin is a competitive inhibitor of glucose transport into erythrocytes (55). One report claims that it is a non-competitive inhibitor of trypanosome glucose transport (56). However, this conclusion was based on measurements of the glycolytic flux, rather than of initial transport, and no data were given. Therefore, the phloretin titrations were simulated, either assuming non-competitive (Fig. 5, *A* and *B*, or competitive inhibition (Fig. 5, *C* and *D*). When non-competitive inhibition was assumed, it was impossible to simulate the data at a low and at a high glucose concentration with the same inhibition constant (Fig. 5, *A* and *B*). With a competitive inhibitor, the model results approached the measurements, with a single inhibition constant (Fig. 5, *C* and *D*). However, to obtain a satisfactory agreement between model and measurements, it was necessary to increase the V_{max} of the glucose transporter above the measured value. This may indicate that the real flux control coefficient of glucose transport at 5 mM glucose is substantially lower than 1, implying that other steps also exert control. The flux control coefficient of the glucose transporter is higher than 0, since the lowest concentration of phloretin already inhibited the flux. All in all, these experiments confirmed the conclusion of the kinetic calculations that the glucose transporter carries significant but not all control.

The Distribution of Control between the Supply and Demand for ATP—A main function of glycolysis is to supply the cell with the ATP necessary for all free energy-requiring processes. This is especially true for bloodstream form trypanosomes in which glycolysis is the only source of ATP. Therefore, it was surprising that the utilization of ATP had no control of the glycolytic flux in the model (Tables III and IV). What caused this lack of control by ATP utilization?

Zooming away from the details, we considered the glycolytic pathway as consisting of two modules: one producing cytosolic ATP (supply) and one consuming it (demand) (20, 50, 51). The only common intermediate connecting these modules is the cytosolic [ATP]/[ADP] ratio. The distribution of control between the supply and demand modules should depend on their relative sensitivity to the common intermediate. The more sensitively a module responds to a changing cytosolic [ATP]/[ADP] ratio, the less control over the flux it should have (see "Materials and Methods" for mathematical details). Therefore, the low control by the demand for ATP can be due to two reasons; either the demand is extremely sensitive to changes of the [ATP]/[ADP] ratio or the supply is hardly sensitive to this ratio. These sensitivities were quantified in terms of elasticity coefficients (Equation 20). When we compared the sensitivities of the supply and the demand module, it turned out that the control by ATP utilization was so low because the supply rate of ATP was held totally insensitive to the [ATP]/[ADP] ratio. The elasticity coefficient of the latter was lower than 10^{-3} at [ATP]/[ADP] ratios between 1 and 8. Thus, the supply module could not respond to changes of ATP utilization. Due to the compartmentalization of glycolysis, the cytosolic [ATP]/[ADP] ratio is only sensed by PYK. Not only was PYK itself only weakly sensitive to the [ATP]/[ADP] ratio (its elasticity coefficient was -0.24 at 5 mM extracellular glucose), but it also had little control on the flux through the supply module (less than 0.2%). Even if PYK was made more sensitive to the [ATP]/[ADP] ratio (an elasticity coefficient of -0.9) by including product inhibition by ATP (Equation 3), this was not transmitted to the rest of the supply module due to the low control by this enzyme (still less than 2%). One way to increase the control of the supply flux by PYK and concomitantly to increase the flux control by the demand reaction was to decrease the V_{max} of PYK to below 156 nmol min^{-1} mg of $protein^{-1}$ in the absence of product inhibition or below 780 nmol min^{-1} mg of $protein^{-1}$ with product inhibition. However, this is only 6 or 30%, respectively, of the activity measured by two independent groups (7, 47). It seems more likely that our calculation that there resides little control in PYK and ATP utilization is realistic.

How Can Trypanosome Glycolysis Be Inhibited Effectively?—One intended application of this study is the identification of the best drug targets of trypanosome glycolysis. Table V reports the extent to which each enzyme had to be inhibited for the glycolytic flux to drop by 50%. The glucose transporter appeared to be the most promising candidate target, since only 51% inhibition of the transporter sufficed to inhibit the flux by 50%. ALD, GDH, GAPDH, and PGK, enzymes that under some conditions shared control, were intermediate candidates. Surprisingly, HK, PFK, and PYK, enzymes that are often thought to control glycolysis, were the poorest candidates from this perspective. They had to be inhibited by 93% or more to reduce the flux by 50%. To investigate whether these enzymes were present in excess, it was also calculated which enzyme inhibition was required for a 10% inhibition of the flux (Table V). Again, glucose transport was the most effective drug target, followed by ALD, GAPDH, GDH, and PGK. Indeed HK, PFK, and PYK appeared to have a huge overcapacity.

DISCUSSION

This study has addressed the question of which steps control the glycolytic flux in bloodstream form *T. brucei.* The unique situation that a sufficiently complete set of kinetic data is available for a single condition made it possible to calculate an

TABLE III

The control of the glycolytic flux (C_i^J) and the displacement from equilibrium (Γ/K_{eq}) under aerobic conditions

Flux control coefficients were calculated according to Equation 18. The displacement from equilibrium was quantified as the actual ratio of product to substrate concentrations (Γ) divided by the equilibrium constant (K_{eq}). The extracellular glucose concentration was varied between its physiological boundaries. The most common blood glucose concentration is 5 mM. Control coefficients above 5% have been set in boldface.

Reaction	4 mM glucose		5 mM glucose		8 mM glucose	
	C_i^J	Γ/K_{eq}	C_i^J	Γ/K_{eq}	C_i^J	Γ/K_{eq}
	%		%		%	
Glucose transport	**95**	$5.5 \cdot 10^{-3}$	**90**	$6.1 \cdot 10^{-3}$	**63**	$9.2 \cdot 10^{-3}$
HK	2	$\ll 10^{-3}$	2	$\ll 10^{-3}$	4	$\ll 10^{-3}$
PFK	0	$\ll 10^{-3}$	0	$\ll 10^{-3}$	1	$\ll 10^{-3}$
ALD	1	0.25	2	0.22	**10**	0.17
GAPDH	1	0.25	2	0.23	**9**	0.20
PGK	1	$9.5 \cdot 10^{-3}$	2	$7.2 \cdot 10^{-3}$	**6**	$3.4 \cdot 10^{-3}$
PYK	0	$\ll 10^{-3}$	0	$\ll 10^{-3}$	1	$\ll 10^{-3}$
Pyruvate transport	0	$\ll 10^{-3}$	0	$\ll 10^{-3}$	0	$\ll 10^{-3}$
GDH	1	$8.0 \cdot 10^{-3}$	2	$8.4 \cdot 10^{-3}$	**6**	$9.1 \cdot 10^{-3}$
Glycerol-3-phosphate oxidase	0	$\ll 10^{-3}$	0	$\ll 10^{-3}$	1	$\ll 10^{-3}$
ATP utilization	0		0		0	

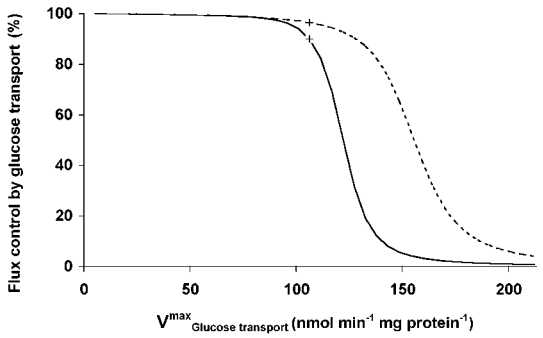

FIG. 4. **The flux control coefficient of the glucose transporter sharply decreases with increasing transport activity.** These results were obtained at 5 mM extracellular glucose. The *solid lines* represent aerobic conditions, and the *dashed lines* anaerobic conditions. The markers indicate the default forward V_{max} (106.2 nmol min^{-1} (mg of protein)$^{-1}$) at which all of the above results were obtained. The forward and reverse V_{max} were varied proportionally to avoid violation of the equilibrium constant.

TABLE IV

The control of the glycolytic flux (C_i^J) and the displacement from equilibrium (Γ/K_{eq}) at increased glucose transport activity

Both the forward and the reverse V_{max} were increased by 35% so that the forward V_{max} became 143.4 nmol min^{-1} mg of protein^{-1}. The extracellular glucose concentration was 5 mM. All other parameters were the same as for Table I. Control coefficients above 5% are given in boldface.

Reaction	C_i^J	Γ/K_{eq}
	%	
Glucose transport	**8**	$6.0 \cdot 10^{-2}$
HK	5	$\ll 10^{-3}$
PFK	1	$\ll 10^{-3}$
ALD	**28**	0.15
GAPDH	**23**	0.21
PGK	**15**	$1.7 \cdot 10^{-3}$
PYK	1	$\ll 10^{-3}$
Pyruvate transport	0	$\ll 10^{-3}$
GDH	**17**	$9.6 \cdot 10^{-3}$
Glycerol-3-phosphate oxidase	2	$\ll 10^{-3}$
ATP utilization	0	

answer to this question. The model that was used in this study was based on this data set and had been validated experimentally (37). The pertinence of our calculations is limited mainly by lack of kinetic information on the metabolite transporters across the glycosomal membrane. If these steps do not operate at equilibrium, as was assumed in this study, the current model overestimates the other flux control coefficients. However, since the glycosome can be considered as a monofunctional unit (49), the ratios of the flux control coefficients of the glycosomal enzymes are not compromised by this uncertainty.

The results presented in this study are at variance with the deceptive consensus in the literature that glucose transport is *the* rate-limiting step of trypanosome glycolysis (17, 29, 43, 56), for the control of glycolysis by the glucose transporter was less than complete, and it depended considerably on both the extracellular glucose concentration and the enzyme activities. A steep shift of control was calculated upon varying the activity of the glucose transporter itself (Fig. 4). Further calculations revealed that this sudden drop of control resulted from the large difference between the K_m values of the glucose transporter (2 mM) and HK (0.1 mM) for intracellular glucose in this model (57). Also an increase of the "apparent" K_m of HK for glucose by a decrease of its K_m for the product Glc-6-P weakened the dependence of the control by the transporter on transporter activity (result not shown). However, the K_m of 12 mM for Glc-6-P that was used here is the lowest K_m that could be reconciled with all kinetic studies reported so far. This suggests that the strong shift of control may well occur in living trypanosomes. Would it also occur in the host cells? In mammalian cells, the difference between the K_m values of glucose transport and HK is similar to that in trypanosomes or even more extreme (58–60). Indeed, a shift of control has been observed in perfused rat heart upon stimulation of the transporter by insulin (36). Insulin may, however, cause a large change of the transport activity, and it is not known whether a small change of the transport activity is sufficient to cause the decrease of control, as it did in the trypanosome model. It may be expected that the shift of control is less abrupt in mammalian cells than in trypanosomes, since the affinity of mammalian hexokinase I, II, and III toward Glc-6-P is very high (59).

Our calculations used a single kinetic equation for the utilization of ATP, obscuring the variety of processes in which ATP is consumed. Ideally, if one of these processes is activated due to a change of the extracellular conditions, the others should not slow down, but the supply of ATP, *i.e.* the glycolytic flux, should adjust to the altered demand (20, 21). The cell can achieve this either by making the supply very sensitive to the cytosolic [ATP]/[ADP] ratio or by making the demand reactions very insensitive to this ratio. The former strategy ensures at the same time homeostasis of the cytosolic [ATP]/[ADP] ratio. Hofmeyr and Cornish-Bowden (51) argued that "the regulatory performance of the system can be judged in terms of how sensitive the fluxes respond to the external stimulus and to what degree homeostasis in the concentrations of the internal regulators is maintained." In the case discussed here, this external stimulus could be anything changing the demand for ATP, and the internal regulator is the cytosolic [ATP]/[ADP] ratio. By this criterion, trypanosome glycolysis worked as a

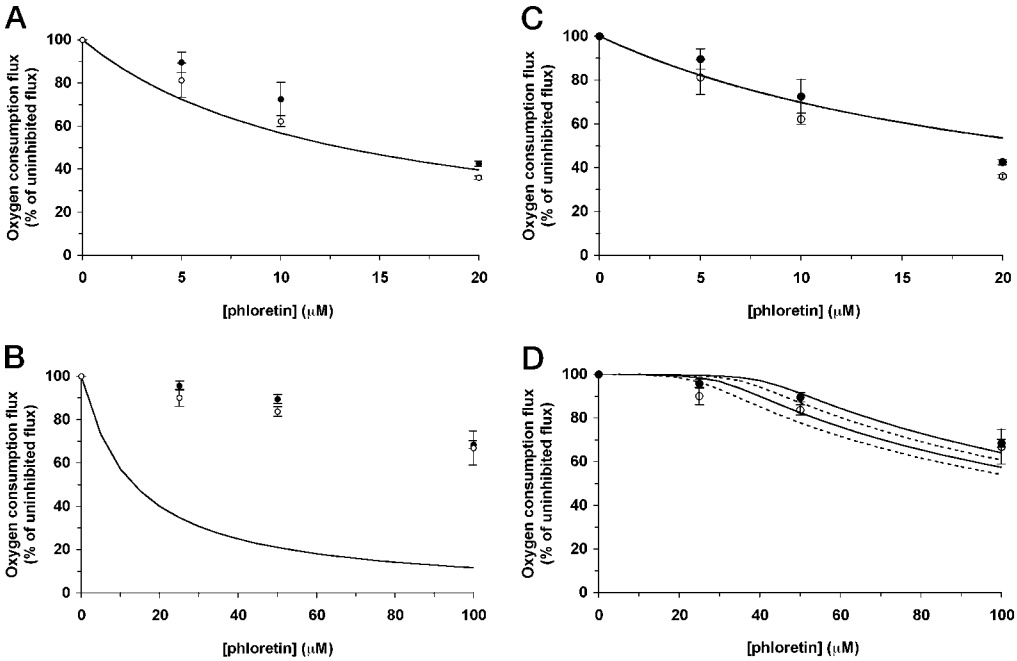

FIG. 5. **Inhibition of glucose transport by phloretin.** The rate of oxygen consumption was measured (*circles*) and simulated (*lines*) at various concentrations of the glucose transport inhibitor phloretin and both at 0.5 mM (*A* and *C*) and 5 mM glucose (*B* and *D*). *Open* and *closed symbols* represent independent experiments with trypanosomes isolated from different rats. In *A* and *B*, it was assumed in the simulations that the inhibition was non-competitive, with a K_i of 13 μM, and at the default V_{max} of glucose transport (106.2 nmol min^{-1} mg of protein^{-1}). In *C* and *D*, competitive inhibition with a K_i of 18 μM was simulated, and the V_{max} of glucose transport was, respectively, 160 (*highest line* in *D*), 170, 180, and 190% (*lowest line* in *D*) of the default value of 106.2 nmol min^{-1} mg of protein^{-1}. At 0.5 mM glucose (*C*), the inhibition curves at different V_{max} values overlapped.

TABLE V
The inhibition of each individual enzyme required to inhibit the flux by 10 and 50%

These results were obtained at 5 mM glucose under aerobic conditions and at constant values of all other enzyme activities. The forward and reverse V_{max} were varied simultaneously by the same percentage.

Reaction	Inhibition required	
	10% flux reduction	50% flux reduction
	%	
Glucose transport	11	51
HK	77	93
PFK	87	93
ALD	44	76
GAPDH	53	84
PGK	61	85
PYK	94	97
GDH	56	83

poor regulatory performer; the control by demand was very low because the supply module hardly sensed the cytosolic [ATP]/[ADP] ratio.

This result raises the question of whether homeostasis of the [ATP]/[ADP] ratio is unimportant for bloodstream form trypanosomes. Alternatively, if homeostasis is important, are these cells unable to cope with changes of their environment that affect the demand for ATP? Trypanosomes living in the bloodstream enjoy a relatively constant environment. Probably the most dramatic event these trypanosomes experience is the transfer from the mammalian bloodstream to the midgut of the tsetse fly. The "long slender" bloodstream form, which is dominant in the blood, does not survive this sudden transfer. Only the intermediate "short stumpy" bloodstream form is able to adapt to the new environment (61). Our calculations predicted that a 90% decrease of the activity of PYK was required to shift the control to the demand for ATP. Perhaps fructose 2,6-bisphosphate, a potent activator of PYK, plays an important role in the transition from the long slender to the intermediate form of *T. brucei*. In bloodstream form trypanosomes, PYK is saturated with fructose 2,6-bisphosphate (12, 16). An interesting test of this hypothesis is to measure whether the intermediate "short stumpy" form of *T. brucei* has a strongly reduced concentration of fructose 2,6-bisphosphate and, consequently, a higher control by the demand for ATP.

The present study has strong implications for the design of anti-trypanosomal drugs; inhibition of the transport of glucose into the cells should be much more effective than inhibition of any of the other steps. Until now the design and synthesis of inhibitors of trypanosome glycolysis has been focused on the enzymes GAPDH (62–67), PGK (68), and ALD (63). According to our model calculations, inhibition of these steps should be less effective than inhibition of glucose transport but far more effective than inhibition of HK, PFK, or PYK. Does this imply that all effort should be shifted to the synthesis of inhibitors of glucose transport? No, some certainly, but not all; the difference of effectiveness between inhibition of GAPDH and inhibition of the glucose transporter may be overcome by the design of an inhibitor of GAPDH or PGK that is 2-fold more effective at the level of the single protein. The real gain of our method may not be an increase of effectiveness but rather an increase of selectivity. If one optimizes the selectivity of the inhibitor at the enzyme level, the inhibition of the host enzyme may be only weak. If, on top of this, the enzyme of interest has a much lower flux control in the host than in the parasite, the compound should inhibit the flux manifold more selectively than it inhibits the single enzyme. From an elaborate model of erythrocyte glycolysis, it was concluded that a 95% deficiency of ALD, GAPDH, or PGK should not cause any clinical symptoms (69). Since these enzymes exerted flux control in trypanosomes, drugs directed against these enzymes have a high probability of being selective against trypanosome glycolysis.

Acknowledgments—We thank S. Marché and J. van Roy for the sharing of unpublished results and B. Teusink and K. van Dam for careful reading of the manuscript and fruitful discussions.

REFERENCES

1. Opperdoes, F. R. (1987) *Annu. Rev. Microbiol.* **41,** 127–151
2. Michels, P. A. M., and Hannaert, V. (1994) *J. Bioenerg. Biomembr.* **26,** 213–219
3. Hannaert, V., and Michels, P. A. M. (1994) *J. Bioenerg. Biomembr.* **26,** 205–212
4. Bakker, B. M., Westerhoff, H. V., and Michels, P. A. M. (1995) *J. Bioenerg. Biomembr.* **27,** 513–525
5. Opperdoes, F. R., and Borst, P. (1977) *FEBS Lett.* **80,** 360–364
6. Visser, N., Opperdoes, F. R., and Borst, P. (1981) *Eur. J. Biochem.* **118,** 521–526
7. Hammond, D. J., Aman, R. A., and Wang, C. C. (1985) *J. Biol. Chem.* **260,** 15646–15654
8. Hammond, D. J., and Bowman, I. B. R. (1980) *Mol. Biochem. Parasitol.* **2,** 77–91
9. Hammond, D. J., and Bowman, I. B. R. (1980) *Mol. Biochem. Parasitol.* **2,** 63–75
10. Eisenthal, R., and Panes, A. (1985) *FEBS Lett.* **181,** 23–27
11. Van Schaftingen, E., Opperdoes, F. R., and Hers, H.-G. (1985) *Eur. J. Biochem.* **153,** 403–406
12. Callens, M., Kuntz, D. A., and Opperdoes, F. R. (1991) *Mol. Biochem. Parasitol.* **47,** 19–30
13. Callens, M., and Opperdoes, F. R. (1992) *Mol. Biochem. Parasitol.* **50,** 235–244
14. Cronin, C. N., and Tipton, K. F. (1987) *Biochem. J.* **245,** 13–18
15. Cronin, C. N., and Tipton, K. F. (1985) *Biochem. J.* **227,** 113–124
16. Van Schaftingen, E., Opperdoes, F. R., and Hers, H.-G. (1987) *Eur. J. Biochem.* **166,** 653–661
17. Gruenberg, J., Sharma, P. R., and Deshusses, J. (1978) *Eur. J. Biochem.* **89,** 461–469
18. Kacser, H., and Burns, J. A. (1973) *Symp. Soc. Exp. Biol.* **27,** 65–104
19. Heinrich, R., and Rapoport, T. A. (1974) *Eur. J. Biochem.* **42,** 89–95
20. Westerhoff, H. V., and Van Dam, K. (1987) *Thermodynamics and Control of Biological Free-energy Transduction*, Elsevier, Amsterdam
21. Fell, D. A. (1997) in *Understanding the Control of Metabolism* (Snell, K., ed) Portland Press, London
22. Kholodenko, B. N., Molenaar, D., Schuster, S., Heinrich, R., and Westerhoff, H. V. (1995) *Biophys. Chem.* **56,** 215–226
23. Burns, J. A., Cornish-Bowden, A., Groen, A. K., Heinrich, R., Kacser, H., Porteous, J. W., Rapoport, S. M., Rapoport, T. A., Stucki, J. W., Tager, J. M., Wanders, R. J. A., and Westerhoff, H. V. (1985) *Trends Biochem. Sci.* **10,** 16
24. Groen, A. K., Wanders, R. J. A., Westerhoff, H. V., Van der Meer, R., and Tager, J. M. (1982) *J. Biol. Chem.* **257,** 2754–2757
25. Poolman, B., Bosman, B., Kiers, J., and Konings, W. (1987) *J. Bacteriol.* **169,** 5887–5890
26. Ruijter, G. J. G., Postma, P. W., and Van Dam, K. (1991) *J. Bacteriol.* **173,** 6184–6191
27. Jensen, P. R., Westerhoff, H. V., and Michelsen, O. (1993) *EMBO J.* **12,** 1277–1282
28. Snoep, J. L., Arfman, N., Yomano, L. P., Westerhoff, H. V., Conway, T., and Ingram, L. O. (1996) *Biotechnol. Bioeng.* **51,** 190–197
29. Ter Kuile, B. H., and Opperdoes, F. R. (1991) *J. Biol. Chem.* **266,** 857–862
30. Michels, P. A. M. (1988) *Biol. Cell* **64,** 157–164
31. Schaaff, I., Heinisch, J., and Zimmermann, F. (1989) *Yeast* **5,** 285–290
32. Davies, S. E. C., and Brindle, K. M. (1992) *Biochemistry* **31,** 4729–4735
33. Kruckeberg, A. L. (1996) *Arch. Microbiol.* **166,** 283–292
34. Kholodenko, B. N., and Brown, G. C. (1996) *Biochem. J.* **314,** 753–760
35. Shulman, R. G., Bloch, G., and Rothman, D. L. (1995) *Proc. Natl. Acad. Sci. U. S. A.* **92,** 8535–8542
36. Kashiwaya, Y., Sato, K., Tsuchiya, N., Thomas, S., Fell, D. A., Veech, R. L., and Passonneau, J. V. (1994) *J. Biol. Chem.* **269,** 25502–25514
37. Bakker, B. M., Michels, P. A. M., Opperdoes, F. R., and Westerhoff, H. V. (1997) *J. Biol. Chem.* **272,** 3207–3215
38. Lanham, S. M. (1968) *Nature* **218,** 1273–1274
39. Kiaira, J. K., and Njogu, M. R. (1994) *Biotechnol. Appl. Biochem.* **20,** 347–356
40. Lowry, O. H., Rosebrough, N. J., Farr, A. L., and Randall, R. J. (1951) *J. Biol. Chem.* **193,** 265–275
41. Bergmeyer, H. U. (1974) *Methods of Enzymatic Analysis*, Verlag Chemie, Weinheim
42. Visser, N., and Opperdoes, F. R. (1980) *Eur. J. Biochem.* **103,** 623–632
43. Eisenthal, R., Game, S., and Holman, G. D. (1989) *Biochim. Biophys. Acta* **985,** 81–89
44. Stanbury, J. B., Wyngaarden, J. B., Frederickson, D. F., Goldstein, J. L., and Brown, M. S. (1993) *The Metabolic Basis of Inherited Disease*, 5th Ed., McGraw-Hill Book Co., New York
45. Misset, O., Bos, O. J. M., and Opperdoes, F. R. (1986) *Eur. J. Biochem.* **157,** 441–453
46. Nwagwu, M., and Opperdoes, F. R. (1982) *Acta Trop.* **39,** 61–72
47. Barnard, J. P., and Pedersen, P. L. (1988) *Mol. Biochem. Parasitol.* **31,** 141–148
48. Fairlamb, A. H., Opperdoes, F. R., and Borst, P. (1977) *Nature* **265,** 270–271
49. Rohwer, J. M., Schuster, S., and Westerhoff, H. V. (1996) *J. Theor. Biol.* **179,** 213–228
50. Schuster, S., Kahn, D., and Westerhoff, H. V. (1993) *Biophys. Chem.* **48,** 1–17
51. Hofmeyr, J.-H. S., and Cornish-Bowden, A. (1991) *Eur. J. Biochem.* **200,** 223–236
52. Sauro, H. M., and Fell, D. A. (1991) *Math. Comp. Modelling* **15,** 15–28
53. Frankel, S., and Reitman, S. (eds) (1963) *Gradwohl's Clinical Laboratory Methods and Diagnosis*, 6th Ed., Vol. 1, C.V. Mosby Co., St. Louis
54. Henry, R. J., Cannon, D. C., and Winkelman, J. W. (eds) (1974) *Clinical Chemistry Principles and Techniques*, 2nd Ed., Harper & Row Publishers
55. Krupka, R. M., and Devés, R. (1980) *Biochim. Biophys. Acta* **598,** 134–144
56. Seyfang, A., and Duszenko, M. (1991) *Eur. J. Biochem.* **202,** 191–196
57. Bakker, B. M., Michels, P. A. M., and Westerhoff, H. V. (1996) in *BioThermo-Kinetics of the Living Cell* (Westerhoff, H. V., Snoep, J. L., Sluse, F. E., Wijker, J. E., and Kholodenko, B. N., eds) pp. 136–142, BioThermoKinetics Press, Amsterdam
58. Gould, G. W., Thomas, H. M., Jess, T. J., and Bell, G. I. (1991) *Biochemistry* **30,** 5139–5145
59. Colowick, S. P. (1973) in *The Enzymes*, (Boyer, P. D., ed) Vol. 9, pp. 1–48, Academic Press, Inc., New York
60. Mueckler, M. (1994) *Eur. J. Biochem.* **219,** 713–725
61. Giffin, B. F., and McCann, P. P. (1989) *Am. J. Trop. Med. Hyg.* **40,** 487–493
62. Vellieux, F. M. D., Hajdu, J., Verlinde, C. L. M. J., Groendijk, H., Read, R. J., Greenhough, T. J., Campbell, J. W., Kalk, K. H., Littlechild, J. A., Watson, H. C., and Hol, W. G. J. (1993) *Proc. Natl. Acad. Sci. U. S. A.* **90,** 2355–2359
63. Perié, J., Riviere-Alric, I., Blonski, C., Gefflaud, T., Lauth de Viguerie, N., Trinquier, M., Willson, M., Opperdoes, F. R., and Callens, M. (1993) *Pharmacol. Ther.* **60,** 347–365
64. Willson, M., Lauth, N., Perié, J., Callens, M., and Opperdoes, F. R. (1994) *Biochemistry* **33,** 214–220
65. Verlinde, C. L. M. J., Callens, M., Van Calenbergh, S., Van Aerschot, A., Herdewijn, P., Hannaert, V., Michels, P. A. M., Opperdoes, F. R., and Hol, W. G. J. (1994) *J. Med. Chem.* **37,** 3605–3613
66. Van Calenbergh, S., Verlinde, C. L., Soenens, J., De Bruyn, A., Callens, M., Blaton, N. M., Peeters, O. M., Rozenski, J., Hol, W. G., and Herdewijn, P. (1995) *J. Med. Chem.* **38,** 3838–3849
67. Kim, H., Feil, I. K., Verlinde, C. L. M. J., Petra, P. H., and Hol, W. G. J. (1995) *Biochemistry* **34,** 14975–14986
68. Bernstein, B. E., Michels, P. A. M., and Hol, W. G. (1997) *Nature* **385,** 275–278
69. Schuster, R., and Holzhütter, H.-G. (1995) *Eur. J. Biochem.* **229,** 403–418